Large-Scale Thermo-Hydrodynamic Modeling of a Flooded Underground Mine for Geothermal Applications

Ting Bao[1] and Zhen (Leo) Liu[2]
[1]Graduate Assistant, Dept. of Civil and Environmental Engineering, Michigan Technological Univ., 1400 Townsend Dr., Dow 854, Houghton, MI 49931. E-mail: tbao@mtu.edu
[2]Assistant Professor, Dept. of Civil and Environmental Engineering, Michigan Technological Univ., 1400 Townsend Dr., Dillman 201F, Houghton, MI 49931 (corresponding author). E-mail: zhenl@mtu.edu

Abstract: The concept of recovering geothermal energy from water in abandoned underground mines has been gaining momentum worldwide in recent years. This is possibly because mine water and surrounding geologic formations can be used for a higher-grade geothermal reservoir than other low-enthalpy geothermal applications. However, the scientific understanding of this application is still in a preliminary stage, leading to a limited number of detailed numerical simulations involving both hydrodynamics and physical process in porous materials. This paper pioneers large-scale hydrodynamics modeling of mine water coupled with heat transfer between mine water and surrounding geologic formations for geothermal applications. For this purpose, a numerical model was implemented and validated against documented experiments. Based on that, a representative case was simulated to shed light on the question regarding how the buoyancy-driven flow is triggered and maintained by the temperature difference that results from the geothermal gradient.

INTRODUCTION

Geothermal energy is one of the alternative energy sources, which provides green and relatively renewable energy for human demands to make the world towards global energy sustainability (Rybach 2003; Lund et al. 2005). One of the attractive applications using geothermal energy is electric power generation considering its advantages such as environment-friendliness and cost-competitiveness over conventional sources of energy (Milora and Tester 1977). Exploring geothermal for the electric power generation needs specific qualifications such as a very high enthalpy fluid or vapor; as a result, only a few countries (24 more or less) can generate electricity by employing geothermal resources (Bertani 2012). Another direct use of geothermal is to heat or cool buildings using geothermal heat pumps (Self et al. 2013). Such apparatus can transfer heat from a low enthalpy source to a high enthalpy fluid via the fluid circulation in heat pumps to boost efficiency for heating /cooling buildings. This type of geothermal application has to drill to access a location of heat stored in the geothermal fields, which is only capable of implementing the extraction of energy from specific areas of the Earth due to economic and technical concerns.

Underground mining is activated in almost every country and a great number of underground mines in numerous counties were closed and abandoned in the past years, many of which were flooded with water after closure (Ramos et al. 2015). Due to this reason, an interesting and valuable question has been proposed that “Can we take the heat

from those abandoned and flooded mines for human demands?" Mine water heated by the Earth's geothermal energy can run through a heat exchanger for humanity's energy needs, which could be an economical, reliable, and environmental option for exploring geothermal energy. Practical attempts have been made to answer this question. A realistic case of using mine water as a large reservoir of heat in Canada was evaluated, and the results of this study confirmed that extraction of energy from mine water in underground mines beneath the community was not only feasible to heat or cool commercial buildings, but also environmental for atmosphere due to a reduction in carbon dioxide emissions (Jessop 1995; Allen et al. 2000). Observations from more investigations also proved that water in closed mines contains a great reserve of geothermal energy (10-50°C) such as in Poland (Malolepszy 2003), Netherlands (Bazargan et al. 2008), Germany (Wieber and Pohl 2008), and Spain (Loredo et al. 2011). Additional efforts have been made on the estimate of thermal output and mine water temperature recovery (Wieber and Pohl 2008), a typical investment and corresponding economic paybacks (Raymond et al. 2008), effective and suitable geothermal energy recovery systems (Hall et al. 2011), effective velocities of mine water (Hasche-Berger 2013), possible environmental impacts (Preene and Younger 2014), and a methodology for implementing mine water-based geothermal heat recovery (Ramos et al. 2015).

The scientific understanding of this topic far lags behind its implementation. Though not extensively, numerical simulations have been adopted to understand the underlying mechanisms. Hamm and Sabet (2010) modeled the hydraulic behavior of the mine reservoir and mine water temperature in a production shaft and revealed the impact of natural convection, the production flow rate, and the permeability of the surrounding rocks on the geothermal potential for exploitations. More efforts are made with the emphasis on critical issues, including the state-of-art challenges of numerical modeling of mine water for geothermal applications (Renz et al. 2009), the locality for extracting the mine water at a required temperature without causing a decrease in the potential of the discharge (Streb and Wieber 2011), and the lifespan of the required temperature supply from mine water (Arias et al. 2014). However, it is still a great challenge to model a flooded underground mine for geothermal energy recovery because of the multiphysical phenomena involved in the process, more specifically, a thermo-hydro-diffuso-chemico-mechanical problem (Liu et al. 2015). This study pioneers a fully coupled 3D model based upon the Finite Volume Element (FVM) to numerically solve the coupled multiphysical processes in the mine water-surrounding geologic formations system, with an aim at understanding natural convection in mine water. The FVM model was validated against documented experiments. Thermo-hydrodynamic modeling of a typical inclined and flooded underground mine shaft in the Upper Peninsula (U.P.) in Michigan was developed to shed light on the primary physical mechanisms underneath the geothermal application using mine water.

3D MODEL DEVELOPMENT

The governing equations of the system involving a multiphysical process are presented in this section. The thermo-hydrodynamic system includes transient natural convective motion of water and heat transfer in the system to describe this multiphysical process. For the natural convective motion of a fluid, the mass of a moving fluid element is conserved by applying the constitutive equation to this element:

$$\frac{\partial \rho}{\partial t} + \nabla \cdot (\rho \mathbf{U}) = 0 \quad (1)$$

where ρ is the fluid density and $\mathbf{U}$ is the velocity. The momentum equation corresponding to the Navier-Stokes equations ensures the conservation of momentum for a fluid element and is described as:

$$\frac{\partial (\rho \mathbf{U})}{\partial t} + \nabla \cdot (\rho \mathbf{U}\mathbf{U}) - \nabla \cdot [\mu_{\text{eff}} (\nabla \mathbf{U} + \nabla \mathbf{U}^T) - \frac{2}{3} \mu_{\text{eff}} (\nabla \cdot \mathbf{U}) I] = -\nabla p_{\text{d}} - \rho_{\text{eff}} \mathbf{g} h_e \quad (2)$$

where μ_{eff} is the effective viscosity and described by $\mu_{\text{eff}} = \mu_{\text{laminar}} + \mu_{\text{turbulent}}$; μ_{laminar} and $\mu_{\text{turbulent}}$ are the laminar dynamic viscosity and turbulent viscosity, respectively; I is the identity matrix; h_e is the elevation. p_{d} is the dynamic pressure, which is corrected by the following equation:

$$p_{\text{d}} = p - \rho \mathbf{g} h_e \quad (3)$$

where p is the total pressure; the absolute value of $\rho \mathbf{g} h_e$ is the static pressure. ρ_{eff} in Eq. 2 is the effective density, which can be represented using the classical Boussinesq approximation in which the relationship between the fluid density and the corresponding temperature is assumed to be linear associated with the coefficient of thermal expansion β:

$$\rho_{\text{eff}} = \rho_{\text{ref}} [1 - \beta (T - T_{\text{ref}})] \quad (4)$$

where ρ_{ref} is the reference density, and T_{ref} is the reference temperature. The energy within the moving fluid element is also conserved and can be written as in terms of enthalpy:

$$\frac{\partial (\rho h)}{\partial t} + \nabla \cdot (\rho \mathbf{U} h) - \nabla \cdot (\alpha_{\text{eff}} \nabla h) = \frac{\partial p}{\partial t} + \mathbf{U} \cdot \nabla p \quad (5)$$

where α_{eff} is the thermal diffusivity which is given by $\alpha_{\text{eff}} = \alpha_{\text{laminar}} + \alpha_{\text{turbulent}}$. h is the specific total enthalpy, which is equal to $h = h_0 + \frac{1}{2}|\mathbf{U}|^2$, where h_0 is the specific enthalpy.

As heat transfer in the surrounding solid regions is coupled, thermal conduction in the solid regions is governed by the equation:

$$\rho_{\text{s}} c_{\text{p}} \frac{\partial T}{\partial t} = \nabla \cdot (k \nabla T) \quad (6)$$

where ρ_{s} is the solid density, c_{p} is the specific heat of the sloid, k is the thermal conductivity of the sloid, and T is the temperature. It is noted that the surrounding solid regions were assumed as solid rocks (non-porous materials) for simplicity and the effect of temperature on the thermal properties of water was neglected in this study.

The governing equations presented above are solved using an open source FVM platform, OpenFoam. Since there is one more variable which is coupled with other variables as shown in Eqs 1 to 6, the efficient way to address such a problem is to solve the

governing equations separately in different regions. The final results then can be obtained via combing results from each part. The details regarding discretization of the governing equations can be found in Ferziger and Peric (2012). The PISO algorithm was used in this study to solve the iteration of the system (J. Oliveira 2001; Ferziger and Peric 2012), which applies very few corrector steps to obtain a desired accuracy of the pressure and velocity. The difference in temperature is relatively small so that the correction of temperature is achieved at each time step by employing the Boussinesq approximation (J. Oliveira 2001). The heat transfer between fluids and surrounding solids is coupled using "baffles" that can emulate transfer thermal energy between both sides of the baffle.

SIMULATION RESULTS AND MODEL VALIDATION

The validation of the developed model in the above section against a documented experiment is presented in this section. Braga and Viskanta (1992) conducted an experiment to investigate transient natural convective heat transfer in water (near its maximum density) in a rectangular cavity with inside dimensions of 150 mm in height, 300 mm in length, and 75 mm in depth. The experiment consisted of three major parts as shown in Fig. 1, i.e., a cold wall in which the temperature was maintained at 273.15 K, a hot wall (opposite to the cold wall) in which the temperature was maintained at 281.15 K, and water between the two walls in which there was a small gap (3 mm) between the top insulation and water to produce a free water surface. The walls around water were insulated and several thermocouples were inserted into the top, middle and bottom of the water body to measure temperature variations with respect to time at these points.

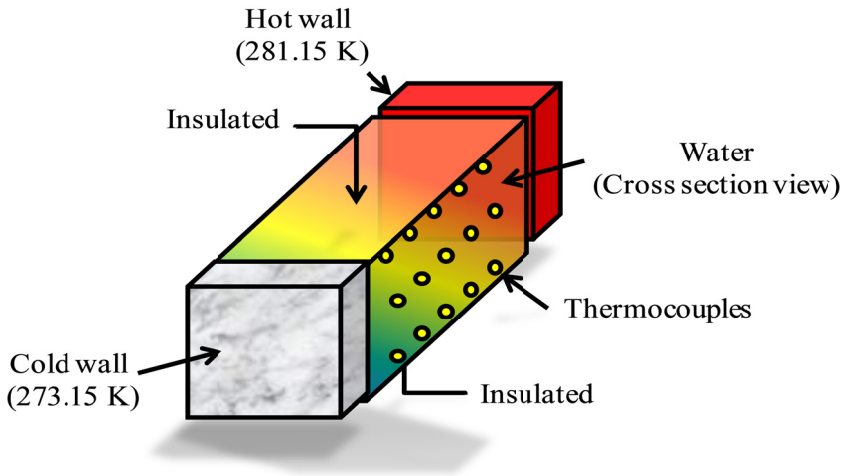

FIG.1. Schematic cross section view of the experiment conducted by Braga and Viskanta (1992).

This experiment was performed to investigate heat transfer and water movement triggered by temperature differences. To visualize the flow patterns, the water was mixed with an amount of neutrally buoyant particles (Braga and Viskanta 1992), which was scanned by the laser beam so that the flow patterns can be visualized through the front and back insulations. The Boussinesq approximation in Eq. 4 is valid in most cases to simulate natural convection as the density of fluids decreases linearly with increasing temperature.

However, this approximation is invalid for this experiment due to the effect of density inversion. To be more special, the maximum density of water appears at 277.13 K so that the density fails to linearly vary with temperature, which significantly affects the natural convective motion at locations near to the density extremum (Braga and Viskanta 1992). In order to accurately simulate this experiment, the relationship between the fluid density and the corresponding temperature was corrected using Eq. 7 (McDonough and Faghri 1994):

$$\begin{cases} \rho_{\text{eff}} = \rho_{\text{ref}}[1+\beta_1 T+\beta_2 T^2+\beta_3 T^3+\beta_4 T^4]^{-1} \\ \rho_{\text{ref}} = 999.972(kg/m^{-3}) \\ \beta_1 = -0.67896452\times10^{-4}(^{\circ}C^{-1}) \\ \beta_2 = 0.907294338\times10^{-5}(^{\circ}C^{-1}) \\ \beta_3 = -0.964568125\times10^{-7}(^{\circ}C^{-1}) \\ \beta_4 = 0.873702983\times10^{-9}(^{\circ}C^{-1}) \end{cases} \tag{7}$$

The initial and boundary conditions in the current simulation were set up according to the real conditions. An initial temperature of 281.15 K was uniformly distributed within the water body. Non-slip was used on all boundaries between the water and walls. For the boundary conditions of flow on the free surface, the velocity normal to the surface was set up zero while zero gradients were defined for velocities in the other directions. Due to the negligible dimensions in the surrounding solids, heat transfer in the solids was not considered in this case. The parameters regarding thermal and transport properties used in the model were adopted from Braga and Viskanta (1992). 78,120 volume cells were generated for the water body and 0.1 s was selected as the time step. Such a mesh and time step were tested and a good accuracy and computing cost were obtained with them.

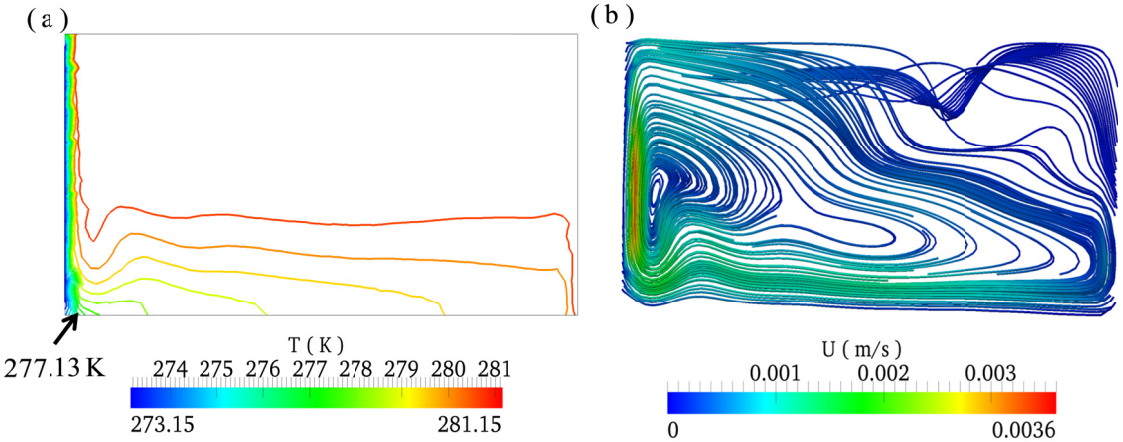

FIG.2. Numerical simulation results on a cross section of height at *t*=5 min: (a) temperature distribution and (b) streamlines.

The water density distribution with temperature in the cavity has been presented in Fig. 2a based upon transient isotherms. The maximum density appears at the 277.13 K isotherm at a location close to the corner, which separates the water body into two parts with

different flow patterns. But during this period, heat conduction was predominant within the water body in the process. Therefore, these two separate parts with different flow patterns in the cavity is not explicit. This result also can be validated by the corresponding transient streamlines presented in Fig. 2b. It can be clearly seen that the flow circulates anticlockwise from the hot wall to the cold wall, which verifies that heat conduction was dominant and convection was initiated during this period. Unfortunately, no results regarding flow patterns were obtained in the experiments during this period.

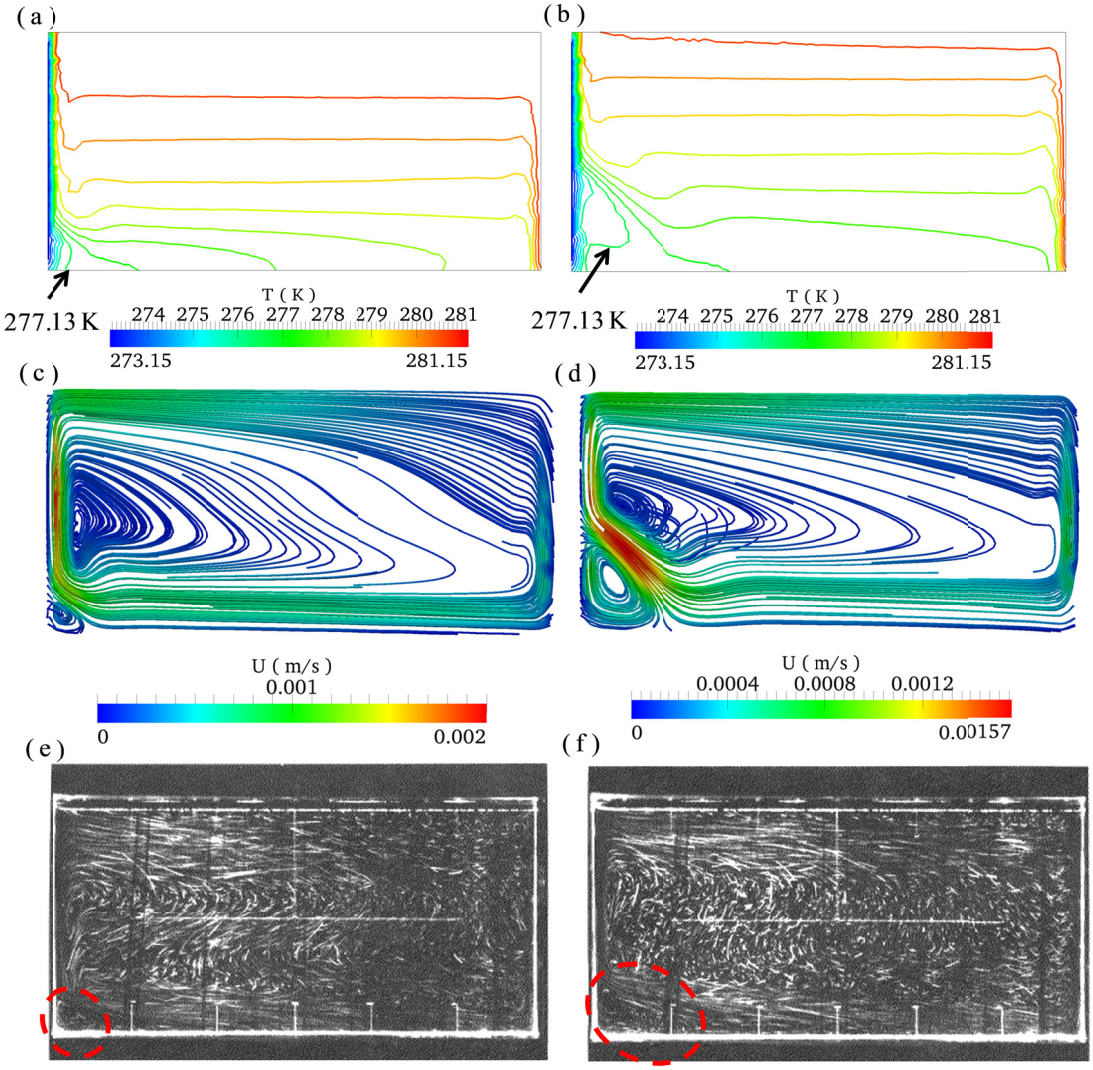

FIG.3. Numerical simulation results on a cross section of height: (a) temperature distributions at *t*=15 min; (b) temperature distributions at *t*=30 min; (c) streamlines at *t*=15 min; (d) streamlines at *t*=30 min; (e) observed streamlines at *t*=15 min; (f) observed streamlines at *t*=30 min (observed photos are copied from Braga and Viskanta (1992)).

Interesting flow patterns caused by natural convection were observed as time elapsed. At *t*=15 min, the fluid that had been cooled to the density inversion (Fig. 3a) exhibited two circulations. One circulation is that the flow along the cold wall at the corner is forced to

move up and then to move down along the 277.13 K isotherm due to buoyancy as shown in Fig. 3c. The other circulation followed a similar flow pattern obtained at t=5 min. The flow patterns at t=15 min show very good agreement with the observed flow patterns in Fig. 3e. This phenomenon is also confirmed by the results obtained at t=30 min in Fig. 3b and Fig. 3d. Due to the heat convection, two separate flow circulations are more obvious. The observed flow patterns in Fig. 3f reaffirm this phenomenon with very a good comparison.

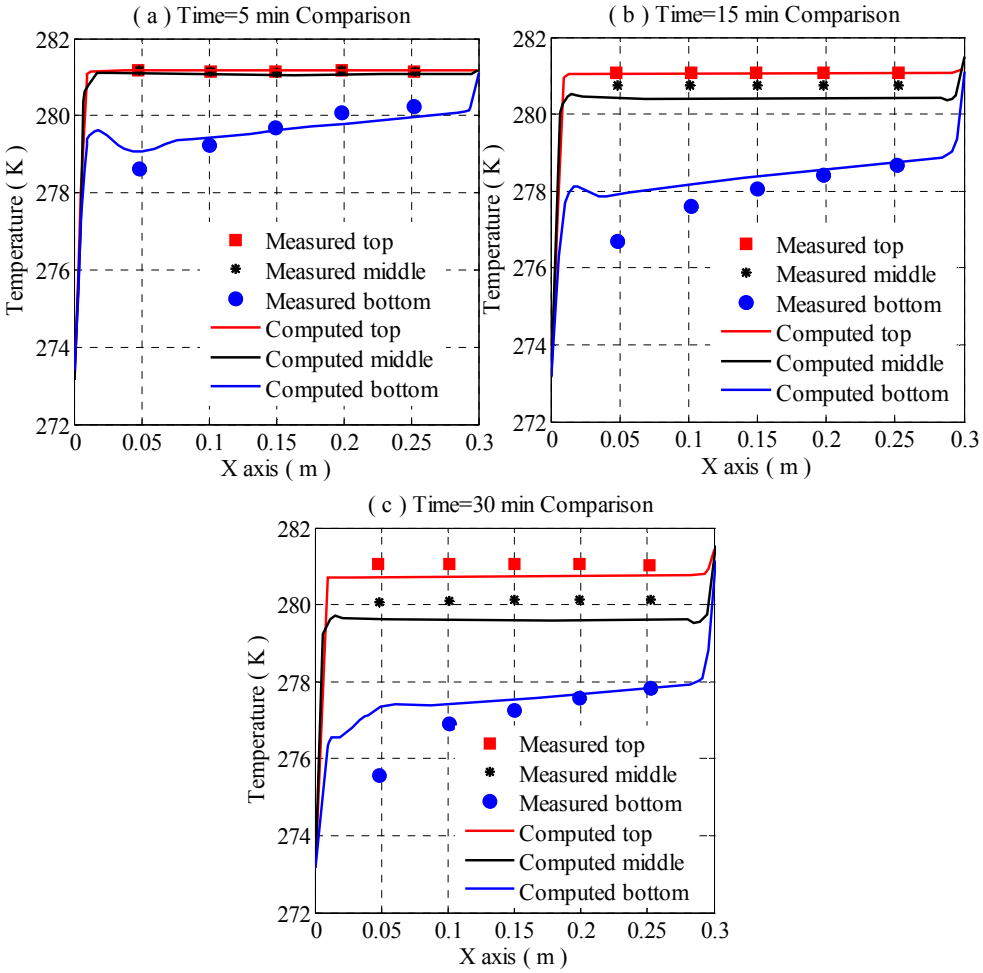

FIG.4. Numerical computed temperatures compared with measured temperatures: (a) t=5 min; (b) t=15 min; and (c) t=30 min (measured data are reproduced from Braga and Viskanta (1992)).

Good comparisons between the computed and measured temperatures further proved the good accuracy of the model. As presented in Fig 4, it can be clearly seen that the distributions of computed temperatures match very well with that of measured temperatures at all different positions for all different times. A slightly difference in the comparison between the computed temperatures and measured temperatures at the bottom was primarily caused by heat conduction along the thermocouple probes (Braga and Viskanta 1992). This heat conduction is particularly significant at locations close to the lower left corner where the density inversion appears. Therefore, the measured temperatures are slightly smaller than the computed values.

SIMULATION OF REPRESENTATIVE CASE

Good comparisons between simulations results and measured data presented in the above section have exhibited the good capacity and accuracy of the proposed 3D FVM model. In this section, a realistic case regarding thermo-hydrodynamic modeling of an inclined and flooded underground mine in the Upper Peninsula (U.P.) in Michigan was investigated to shed light on the understanding of the complicated physical processes in mine water. As reported by Liu et al. (2015), 90% of underground mines were abandoned and flooded with water after closure in the U.P., which results in a huge potential of exploring geothermal energy from those flooded mines to meet the heating demands of the adjacent communities. Therefore, it is of significant meaning and of great interest to study this thermo-hydrodynamic system, with focuses on the transient natural convective motion of water and heat transfer in the system.

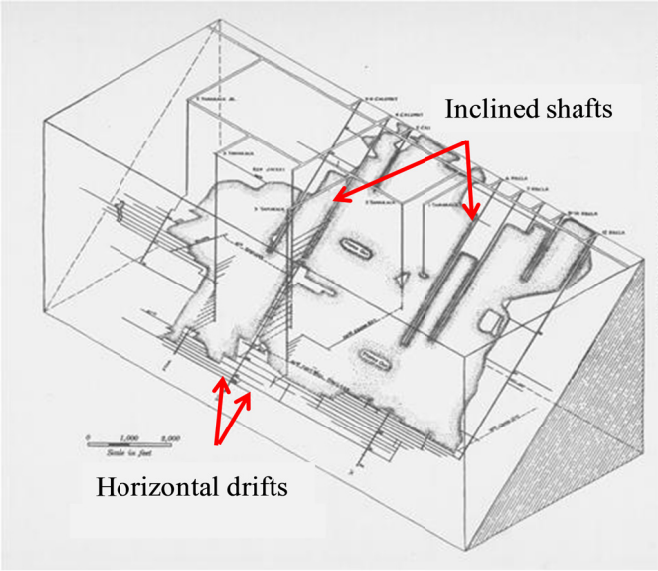

FIG.5. Sketch of a typical underground mine structure (copied from Keweenaw Digital Archives (Book TN443M5V5-002 Figure 1)).

A typical underground mine structure that consists of inclined mine shafts and horizontal drifts connecting those shafts is shown in Fig. 5. For simplicity, an inclined mine shaft was investigated without horizontal drifts as shown in Fig. 6, including information about the computational domain. In order to represent the geothermal gradient in the domain, the temperature was linearly distributed within the water body and surrounding rocks (basalt) from 290 K to 300 K to represent the linear geothermal gradient. The temperature of rocks at the bottom was uniform and fixed to 300 K within the whole domain. In this case, the classical Boussinesq approximation (Eq. 4) can be used due to the absence of density inversion. The interface between different regions was coupled by using "baffles" to simulate heat exchange between two sides of the baffle. Due to a high computing cost in the large-scale simulations, this study presents the results for a process lasting 18 days. The thermal properties of water used in the simulation were chosen at the normal temperature of 299.15 K, and the thermal properties rocks were selected using typical values.

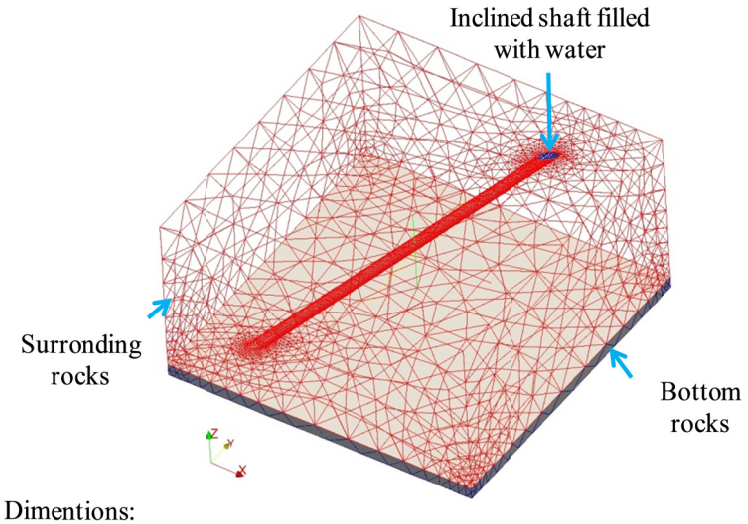

FIG.6. 3D model of the system and its dimensions.

The flow pattern in the center of the water body is depicted in Fig. 7. Due to the density difference caused by the geothermal gradient, the mine water circulates in the shaft, in which the water at the bottom with high temperatures is relatively lighter so that it moves up. Then the water from the bottom is mixed and cooled by the cold water at the top. The cooled water tends to be heavier and therefore moves down and returns to the bottom. This flow phenomenon can be clearly seen in Fig. 7 using flow vectors and streamlines.

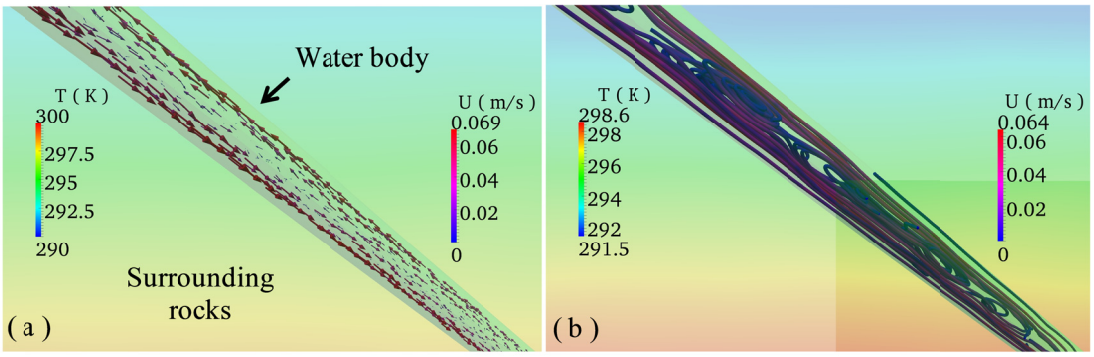

FIG.7. Flow patterns in the center of the water body at t= 1 day: (a) flow circulation and (b) the corresponding streamlines.

The temperature distribution and its variation along the water body are critical to understanding the thermal energy, which triggers and maintains the buoyancy-driven flow. For this purpose, three representative points, which were captured from the surface, middle and bottom of water body, respectively, were chosen to investigate temperature variations with respect to time. As shown in Fig. 8a, the temperature at the bottom decreases

significantly at the beginning and then tends to be uniform. Opposite results were obtained in which the temperature at the top increases significantly at the beginning and then tends to be uniform. The temperature at the middle almost maintains unchanged. These results provide evidence to explain the simulated flow pattern in Fig. 7. The temperature distribution along the water body in Fig. 8b also elucidates what showed in the flow pattern in Fig. 7. The difference between the temperatures on the top and bottom increases from 10 K to 2 K as time elapses. The temperature of mine water is mixed and tends to be uniform gradually due to the natural convective motion of mine water. This well mixing condition is consistent with most field observations in flooded mines (Wolkersdorfer 2008).

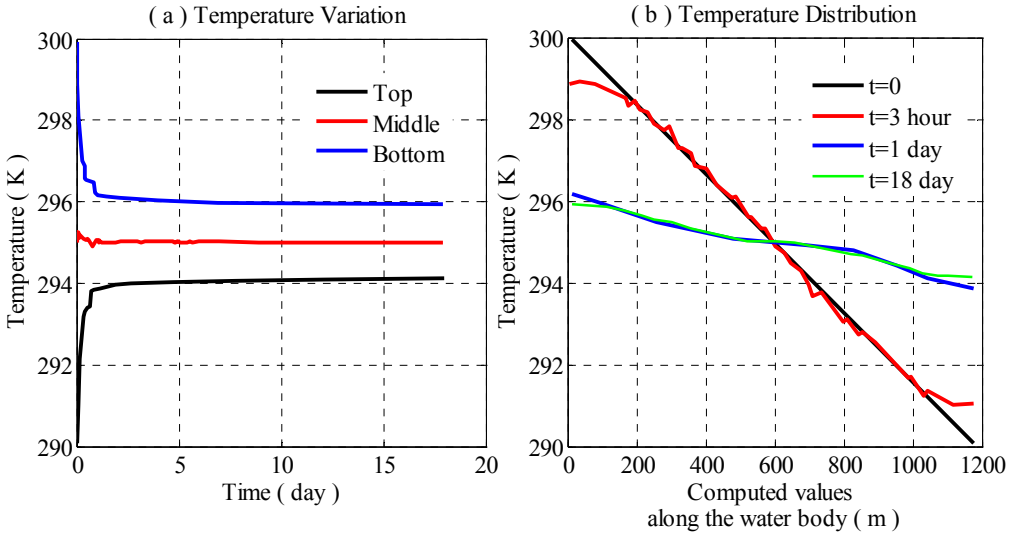

FIG.8. Numerical computed temperatures: (a) temperature variation at different positions, and (b) temperature distribution along the water body.

CONCLUSIONS

A fully coupled 3D thermo-hydrodynamic model was developed using the Boussinesq approximation to numerically solve the coupled mutilphysical processes in the mine water-geologic formation system. The fully coupled 3D model was validated against a documented experiment. Good agreement obtained from the comparison revealed a good accuracy of the developed model. Based on that, a realistic case involving thermo-hydrodynamics of an inclined and flooded underground mine in the Upper Peninsula (U.P.) in Michigan was investigated to shed light on the interesting phenomena in mine water induced by natural convective motion of mine water. The simulation results exhibited how the buoyancy-driven flow is triggered and maintained by the temperature difference in mine water. The results in this study are not only significant to understanding the underlying multiphysics mechanisms associated with recovering geothermal energy from mine water, but also practically valuable to further geothermal applications by efficiently exploring geothermal energy from mine water with more complicated underground mine structures.

REFERENCES

Allen, D., Ghomshei, M., Sadler-Brown, T., Dakin, A., and Holtz, D. (2000). "The current status of geothermal exploration and development in Canada." *Proceedings from World Geothermal Congress*, Japan, 55-58.

Arias, C. A., Alonso, A. O., and García, R. Á. (2014). "Hydrogeological and Thermal Modelling of an Underground Mining Reservoir." In *Mathematics of Planet Earth*, 419-423. Springer.

Bazargan, B., Demollin, E., and Van Bergermeer, J.-J. (2008). "Geothermal use of deep flooded mines." *Proc. of the Post Mining Symposium*, Nancy, France, 1-10.

Bertani, R. (2012). "Geothermal power generation in the world 2005–2010 update report." *Geothermics*, 41: 1-29.

Braga, S., and Viskanta, R. (1992). "Transient natural convection of water near its density extremum in a rectangular cavity." *International journal of heat and mass transfer*, 35(4): 861-875.

Ferziger, J. H., and Peric, M. (2012). *Computational methods for fluid dynamics*. Springer Science & Business Media.

Hall, A., Scott, J. A., and Shang, H. (2011). "Geothermal energy recovery from underground mines." *Renewable and Sustainable Energy Reviews*, 15(2): 916-924.

Hamm, V., and Sabet, B. B. (2010). "Modelling of fluid flow and heat transfer to assess the geothermal potential of a flooded coal mine in Lorraine, France." *Geothermics*, 39(2): 177-186.

Hasche-Berger, A. (2013). "Hydrodynamics in a flooded underground limestone mine." *Reliable Mine Water Technology*, IMWA, Golden CO, USA, 1165-1172.

J. Oliveira, R. I. I., Paulo. (2001). "An improved PISO algorithm for the computation of buoyancy-driven flows." *Numerical Heat Transfer: Part B: Fundamentals*, 40(6): 473-493.

Jessop, A. (1995). "Geothermal energy from old mines at Springhill, Nova Scotia, Canada." *Proceedings*, 463-468.

Liu, Z., Meldrum, J., Xue, P., and Green, C. (2015). "Preliminary Studies of the Use of Abandoned Mine Water for Geothermal Applications." *IFCEE 2015*, ASCE, 1678-1690.

Loredo, J., Ordóñez, A., Jardón, S., and Álvarez, R. (2011). "Mine water as geothermal resource in Asturian coal mining basins (NW Spain)." *Proceedings of 11th International Mine Water Association Congress*, Rüde TR, Freund A, Wolkesdorfer C (eds) Mine water: managing the challenges, Aachen, Germany, 177-182.

Lund, J. W., Freeston, D. H., and Boyd, T. L. (2005). "Direct application of geothermal energy: 2005 worldwide review." *Geothermics*, 34(6): 691-727.

Malolepszy, Z. (2003). "Low temperature, man-made geothermal reservoirs in abandoned workings of underground mines." *Proceedings of the 28th workshop on geothermal reservoir engineering, Stanford University, USA*, 259-265.

McDonough, M., and Faghri, A. (1994). "Experimental and numerical analyses of the natural convection of water through its density maximum in a rectangular enclosure." *International journal of heat and mass transfer*, 37(5): 783-801.

Milora, S. L., and Tester, J. W. (1977). "Geothermal energy as a source of electric power." *Geological Magazine*, 114(5): 1-3.

Preene, M., and Younger, P. (2014). "Can you take the heat?-Geothermal energy in mining." *Mining Technology*, 123(2): 107-118.

Ramos, E. P., Breede, K., and Falcone, G. (2015). "Geothermal heat recovery from abandoned mines: a systematic review of projects implemented worldwide and a methodology for screening new projects." *Environmental Earth Sciences*, 73(11): 6783-6795.

Raymond, J., Therrien, R., and Hassani, F. (2008). "Overview of geothermal energy resources in Québec (Canada) mining environments." *10th International Mine Water Association Congress: mine water and the environment*, Technical University of Ostrava, Ostrava, Czech Republic, 1-12.

Renz, A., Rühaak, W., Schätzl, P., and Diersch, H.-J. (2009). "Numerical modeling of geothermal use of mine water: challenges and examples." *Mine Water and the Environment*, 28(1): 2-14.

Rybach, L. (2003). "Geothermal energy: sustainability and the environment." *Geothermics*, 32(4): 463-470.

Self, S. J., Reddy, B. V., and Rosen, M. A. (2013). "Geothermal heat pump systems: status review and comparison with other heating options." *Applied Energy*, 101: 341-348.

Streb, C., and Wieber, G. (2011). "Geothermal energy from a flooded mine: a hydraulic model." *Rüde RT, Freund A, Wolkersdorfer Ch (Eds), Mine Water–Managing the Challenges, IMWA*: 189-193.

Wieber, G., and Pohl, S. (2008). "Mine water: a source of geothermal energy—examples from the Rhenish Massif." *10th International Mine Water Association Congress: Mine Water and the Environment*, Citeseer, Technical University of Ostrava, Ostrava, Czech Republic, 1-4.

Wolkersdorfer, C. (2008). *Water management at abandoned flooded underground mines: fundamentals, tracer tests, modelling, water treatment*. Springer Science & Business Media.